



Oxidative removal of phenol from water catalyzed by nickel hydroxide

Muhammad Saeed*, Mohammad Ilyas

National Centre of Excellence in Physical Chemistry, University of Peshawar, Peshawar 25120, KPK, Pakistan

ARTICLE INFO

Article history:

Received 2 May 2012

Received in revised form 9 August 2012

Accepted 18 September 2012

Available online 25 September 2012

Keywords:

Phenol

Nickel hydroxide

Kinetic studies

Adsorption isotherms

ABSTRACT

This work explores the preparation and characterization of nickel hydroxide catalyst and investigation of its catalytic activities for oxidative degradation of phenol in aqueous medium using batch reactor. The catalyst was prepared by reaction of sodium hypochlorite, sodium hydroxide and nickel sulfate hexahydrate in distilled water. The prepared catalyst was characterized by surface area, particle size, FTIR, XRD, SEM, and determination of oxygen content measurements. The prepared nickel hydroxide was used as catalyst for oxidative degradation of phenol in aqueous medium by taking 15 mL of 0.71 M phenol solution. The catalytic performance of nickel hydroxide was explored in terms of effect of time, temperature, partial pressure of oxygen, initial concentration of phenol, catalyst loading and effect of stirring speed on degradation of phenol. The catalyst was separated from the reaction mixture by filtration. Langmuir–Hinshelwood type of mechanism was followed in the reaction where adsorption of phenol and oxygen at the surface of catalyst was taking place according to competitive Langmuir and Temkin adsorption isotherm, respectively.

© 2012 Elsevier B.V. All rights reserved.

1. Introduction

Waste water contaminated with phenol has got much attention. As phenol is a basic structural unit for a variety of synthetic organic compounds therefore; wastewater originating from many industries like paper and pulp, resin manufacturing, gas and coke manufacturing, tanning, textile, plastic, rubber, pharmaceutical, and petroleum contain phenol and substituted phenols. Decay of vegetation also contributes phenols to water bodies. Phenols are harmful to organisms and many of them have been classified as hazardous pollutants because of their potential harm to human health. The ingestion of phenols in the human body causes protein degeneration, tissue erosion, and paralysis of the central nervous system and also damages the kidney, liver and pancreas [1,2]. The permissible limit of phenol in water is 4000 µg/L. It is, therefore; important to remove phenols from contaminated industrial aqueous streams before they are discharged into any water body. The effective removal of phenolic pollutants from wastewater is a problem of great importance and interest [3]. Great attention has been given to different alternatives for the removal of phenolic compounds from water. The wet oxidation (WO) process is one of the most convenient, economically and technologically viable solutions over traditional biological process for the removal of organic pollutants like phenols in wastewater [4]. It is the oxidation of both organic and inorganic substances in aqueous solution by means

of oxygen at elevated temperatures (398–593 K) and pressures (0.5–20 MPa). Due to high temperature and pressure, high equipment and operational costs are inevitable, which can be lowered by adding a suitable catalyst either homogenous or heterogeneous type, referred to as catalytic wet oxidation (CWO). Several homogeneous catalysts exhibit good performances for different waste water treatments; however, the metal ions left in the treated water are also a pollutant, which requires additional costly separation process. The problem of this second contamination can be overcome by heterogeneous catalysts and hence this process has gained much attention. Heterogeneous CWO is more promising process for the waste water treatment, using solid supported/unsupported metals/metal oxides as heterogeneous catalysts; where oxygen (air), ozone, hydrogen peroxide, or a combination can be used as the oxidative agent. Heterogeneous wet catalytic process of wastewater has many advantages like easy recovery, regeneration and reuse of the catalyst [5–7]. Several heterogeneous catalysts have been attempted for mineralization of phenolic compounds in aqueous medium [4,8–19]. Complete mineralization of phenol has been achieved over zeolite supported cerium–manganese catalyst, doped with potassium temperature 383 K and 0.5 MPa pressure of oxygen [4]. D.H. Bremner and his co-workers [8] reported heterogeneous sono-Fenton system (Fe_2O_3 , H_2O_2 and ultrasonic radiation) for treatment of phenol in aqueous medium. TiO_2 /activated carbon composite catalyst has been used as catalyst for removal of phenol from aqueous medium by C. Ngamsopasiriskun et al. [9]. It was reported that the percentage removal of 100 ppm phenol by 0.4 g of TiO_2/AC in 4 h was 68.03%, due to both adsorption (54.14%) and catalytic degradation (13.88%). Laoufi et al. [10] and Wang

* Corresponding author. Tel.: +92 91 9216766/346 9010903; fax: +92 91 9216671.

E-mail address: pkseeed2003@yahoo.com (M. Saeed).

et al. [11–13] have also reported TiO_2 as heterogeneous catalyst for degradation of phenol in aqueous medium. $\text{MnO}_2/\text{CeO}_2$ catalyzed WO of phenol in a slurry reactor in the temperature range of 353–403 K and pressure of 2.04–4.76 MPa has been reported by A.J. Luna et al. [14]. The total removal of phenol (2.08 g/L) was achieved within 40 min of reaction at 403 K and a catalyst loading of 6.0 g/L. Lia and his co-workers have reported catalytic degradation of phenol to malonic acid and carbon dioxide over mixed valence nickel oxide, NiO_x [15] and cobalt oxide, Co_2O_3 [16]. Similarly a number of catalysts like $\text{CuO} + \text{ZnO}$, $\text{CuO} + \text{NiO}$ and $\text{CuO}/\text{Al}_2\text{O}_3$ [17], ($\text{La}_{0.8}\text{Sr}_{0.2}$) $\text{Mn}_{0.98}\text{O}_3$ [18], $\text{Fe}_2\text{O}_3/\text{SBA}-15$ [19] have been used for wet catalytic oxidation of phenol in aqueous medium.

Nickel-based oxides have been investigated for several years because they exhibit appreciable catalytic activities, good stabilities and low price. Nickel-based oxides have been used as catalysts for many transformations like oxidation of phenols, alcohols, amines and sulfur compounds [20], benzhydrol and diphenylacetonitrile [21], phenol, formaldehyde and benzyl alcohol [5,22,23], cinamyl alcohol, para-substituted derivatives of benzyl alcohol and secondary benzyl alcohol [24]. In this note nickel hydroxide is reported as catalyst for oxidative degradation of phenol in aqueous medium.

2. Experimental

2.1. Materials

Sodium hypochlorite (Merck), sodium hydroxide (Merck), nickel sulfate hexahydrate (Scharlau), phenol (Acros), silver nitrate (Merck), potassium iodate (Scharlau), potassium iodide (Merck), sodium thiosulfate penta hydrate (Acros) and acetic acid (Merck) were used as received. Nitrogen and oxygen gases were supplied by BOC Pakistan Ltd. and were further purified by passing through traps (C.R.S. Inc. 202268) to remove traces of water and oil.

2.2. Preparation of Catalyst

A mixture of sodium hypochlorite and sodium hydroxide was prepared by adding 42 g of sodium hydroxide in 300 mL of 6% sodium hypochlorite. Another solution was prepared by taking 130 g of nickel sulfate hexahydrate in 300 mL of distilled water. First solution was added drop wise to the second one while stirring continuously at 293 K. The mixture was stirred for further 30 min to ensure complete reaction. The resultant black nickel hydroxide was collected by filtration. The precipitate was washed several times until no chlorine was detected by silver nitrate test. Black nickel hydroxide was dried at 383 K for 24 h. After drying, it was ground and sieved.

2.3. Characterization of the Catalyst

The structural characterization of the fresh and used catalysts was obtained by FTIR, XRD and SEM. The fresh catalyst was characterized by surface area, particle size and oxygen content as well. Particle size analyzer (Analysette 22 Compact, Fritsch, Germany) was used for particle size analysis using wet method of analysis.

BET surface area of the catalyst was determined using a Quanta Chrome (Nova 2200e) surface area and pore size analyzer. Samples were degassed at 383 K for 2 h prior to analysis.

The FTIR spectra were recorded in KBr medium using IR Prestige 21, Shimadzu, Japan instrument in the range of 400–4500 cm^{-1} .

X-ray diffraction (XRD) patterns were recorded using X-ray diffractometer, JEOL (JDX-3532) Japan, using $\text{CuK}\alpha$ radiation with a tube voltage of 40 KV and 20 mA with 2θ ranges from 0 to 70°.

Crystallite size of the catalyst was calculated using Scherer's equation [(equation (1))]:

$$D = \frac{0.9\lambda}{\beta \cos\theta}, \quad (1)$$

where D , λ , β and θ is crystallite size, wave length of $\text{CuK}\alpha$ radiation (1.54 Å), line broadening at half peak width (radian) and Bragg angle (°), respectively.

SEM analyses were carried out by using Scanning Electron Microscope (JOEL-JSM 5910 Japan). For this purpose the catalysts were mounted on the sample stubs and coated with gold foil using gold coating machine (JEOL-JSM-420, Japan). The samples were then automatically analyzed using computer software.

The oxygen content was determined by dissolving about 2 g of potassium iodide in 20 mL of 36% acetic acid solution followed by addition of about 0.2 g of the catalyst. The solution was allowed to stand for 15 min under the atmosphere of molecular nitrogen to liberate iodine. After filtration, the liberated iodine was titrated against 0.1 N sodium thiosulfate solution using starch as indicator. For determination of surface oxygen content about 0.2 g of the catalyst and about 2 g of potassium iodide were added to 15 mL buffer solution of pH 7.1 and was vigorously shaken in atmosphere of molecular nitrogen for 15 min. The reaction mixture was then filtered, acidified with 1 N HCl and the liberated iodine was titrated against 0.1 N sodium thiosulfate solution, using starch as indicator. Following expression was used for determination of oxygen content [5,25,26]:

$$\text{Oxygen}_{(\text{gatmOxygen/gCatalyst})} = \frac{\text{Na}_2\text{S}_2\text{O}_3(\text{mL}) \times N(\text{Na}_2\text{S}_2\text{O}_3)}{1000 \times \text{Catalyst(g)} \times 2}. \quad (2)$$

2.4. Degradation protocol

Batch oxidative degradation experiments of phenol using nickel hydroxide as catalyst were carried out at three different temperatures (313, 323, 333 K) at pH 2.5. For a typical run, 15 mL of 0.71 M phenol solution (10 mmol) was taken in reactor and the temperature of the reaction mixture was kept constant at a desired value by the help of hot plate. Molecular oxygen was passed through the solution at the rate of 60 mL per minute. Prior to passing the oxygen through reaction mixture, it was saturated with phenol solution by passing it through saturator containing the same concentration of phenol solution at temperature of condenser (277–281 K). This saturation of oxygen with phenol solution minimizes the loss of reaction mixture from reactor with flow of oxygen. After getting the desired temperature, 1 mL sample was taken to determine any change in the phenol concentration during the heating period. Then 0.2 g catalyst was added to reactor and stirred the reaction mixture continuously. At appropriate time interval reaction was stopped and catalyst was separated from reaction mixture by filtration. Analysis of the reaction mixture was carried out by HPLC (Agilent Technologies) and UV-visible spectrophotometer (Shimadzu UV-160A, Japan). The percent degradation of phenol was calculated using following expression:

$$\text{Conversion}(\%) = \frac{[\text{PhOH}]_0 - [\text{PhOH}]_t}{[\text{PhOH}]_0} \times 100, \quad (3)$$

where $[\text{PhOH}]_0$ is the initial concentration and $[\text{PhOH}]_t$ is the concentration of phenol at the end of each run.

3. Results and discussions

3.1. Characterization of catalyst

BET surface area for fresh and used catalysts were found as 87 and 89 $\text{m}^2 \text{g}^{-1}$, respectively. Slight increase in the surface area of

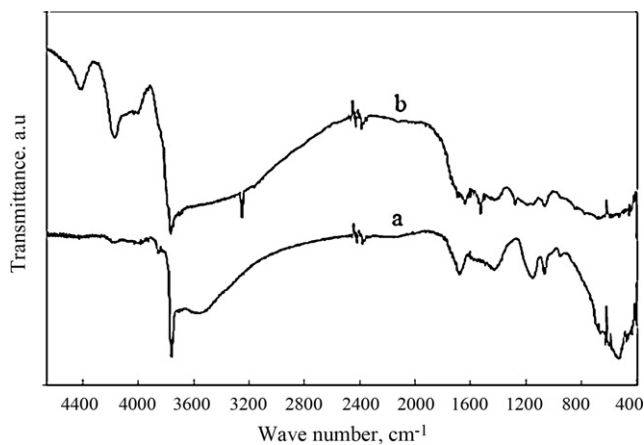


Fig. 1. FTIR spectra of the catalysts. (a) Fresh; (b) Used.

the used catalyst is due to complete dispersion of the particles by stirring in suspension. Porosity was estimated by BJH method considering the desorption branch of nitrogen isotherm. Average pore volume and average pore diameter were 0.04 cc g^{-1} and 24.1 \AA , respectively. Diameter of the 90% pores is $\geq 24.1 \text{ \AA}$. Particle sizes determined by wet method of analysis were in the range of 1–10 μm .

Various bands can be observed in FTIR spectra of the catalysts as given in Fig. 1. Bands in range 480–680, 1500–1700 cm^{-1} were assigned to Ni–O bond and physiosorbed water molecules, respectively. The band at 3698 cm^{-1} was attributed to OH group coordinated to nickel. A small absorption band at $\sim 2400 \text{ cm}^{-1}$ could be due to the physically adsorbed carbon dioxide [25,27]. In the spectrum of used catalyst, this band was pronounced because more carbon dioxide was adsorbed which was formed as result of degradation of phenol. Peaks at 1590, 1381 and 1358 cm^{-1} in spectrum of used catalyst (spectrum b) were assigned to $(\text{COO}^-)\nu_s$, $(\text{CH})\nu$ and $(\text{COO}^-)\nu_{as}$, respectively, which represent malic acid and formic acid formed as a result of degradation of phenol. Band at 3200 cm^{-1} was attributed to phenolic OH group [28–32]. Analyses of the reaction mixture by HPLC also proved the production of these by-products.

The XRD patterns of the catalyst are given in the Fig. 2. These patterns are dominated by sharp and intensive diffraction peaks corresponding to hexagonal crystalline structure. The crystallite size calculated by Scherer's equation was 6.2 nm [5,25]. There is no change in the XRD pattern of fresh and used catalyst, which indicates that the nature of the catalyst doesn't change in the catalytic experiments. On the basis of comparison of FTIR and XRD

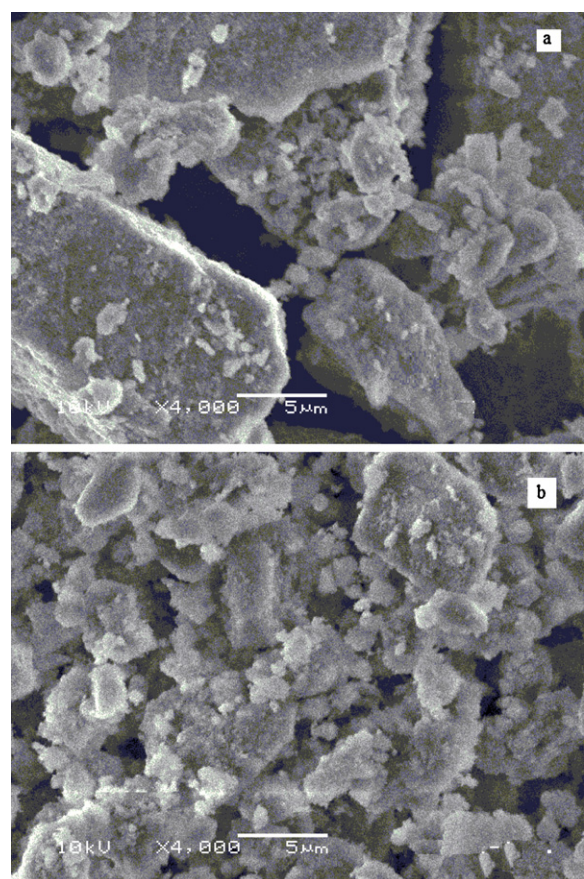


Fig. 3. SEMs of the catalysts. (a) Fresh; (b) Used.

with reported results, it was concluded that the catalyst is Ni(OH)_2 in nature.

SEM shows the homogeneity of the particle's shape (Fig. 3). The SEM of the used catalyst shows that particles are smaller in size and more agglomerated than fresh catalyst. The SEM shows that the particle sizes of the nickel hydroxide catalyst are in the range of micron size.

The total and surface oxygen content of the nickel hydroxide were 3.5×10^{-4} and $2.9 \times 10^{-4} \text{ g-atom oxygen g}^{-1}$ of nickel hydroxide, respectively.

3.2. Oxidation/degradation

The percent degradation of phenol over nickel hydroxide catalyst is plotted in Fig. 4 as function of time at different temperatures. This investigation was carried out with 0.71 M as the initial concentration of phenol, catalyst loading of 0.2 g at 101 kPa partial pressure of oxygen while stirring the reaction mixture at speed of 600 rpm. Separate experiments were carried out for each time-interval investigation. As it is clear in figure that temperature greatly affect the activity for phenol conversion. Ultimately phenol was completely degraded to carbon dioxide and water; however, existence of malic and formic acid was noted which were then mineralized to carbon dioxide and water. This was confirmed by oxidation of malic and formic acid under similar conditions. Formation of carbon dioxide was confirmed by lime-water test. Existence of malic and formic acid detected by HPLC show the oxidative degradation of phenol in present investigation.

To assess the extent of the thermal degradation of phenol, tests were performed with an initial phenol concentration of 0.71 M, in the absence of the heterogeneous catalyst, at temperatures of 313,

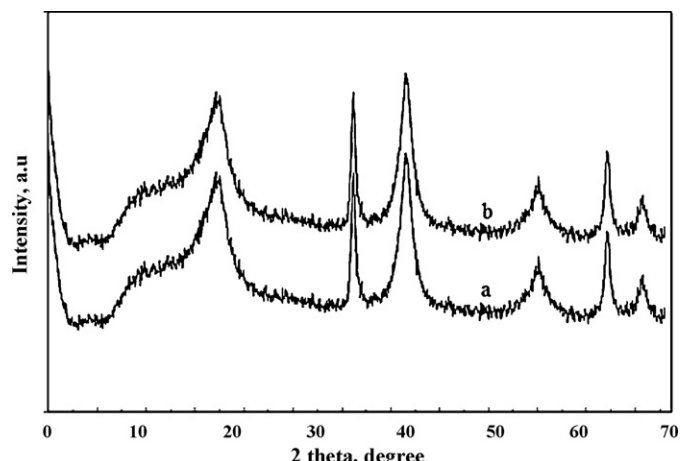


Fig. 2. XRD pattern of the catalysts. (a) Fresh; (b) Used.

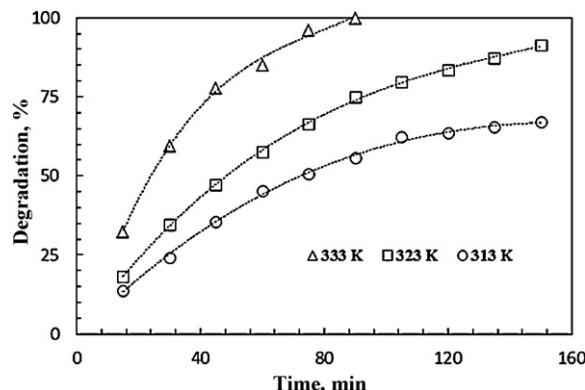


Fig. 4. Time profile of oxidation/degradation of phenol over nickel hydroxide catalyst at various temperatures. Reaction conditions: Phenol 0.71 M (15 mL), Partial pressure of oxygen 101 kPa, Catalyst 0.2 g, Stirring speed 600 rpm.

323 and 333 K for 60 min, while the pressure of oxygen was 101 kPa. Results revealed that there is no appreciable change in concentration of phenol. These investigations showed that nickel hydroxide acts as an effective catalyst for abatement of phenol in aqueous medium.

Leaching of the catalyst is an obstacle in reactions, where reactants in liquid phase and catalyst in solid phase is involved. To test whether leaching of the catalyst in present case is taking place or not, following experiment was performed. First 15 mL water, the solvent, and 0.2 g catalyst were taken in reactor and stirred at 323 K for 1 h. Secondly, the catalyst was separated by filtration and 10 mmol phenol (the reactant) was added. Finally, oxygen was passed through the mixture at the rate of 60 mL/min and stirred at speed of 600 rpm while keeping the temperature constant at 323 K for 1 h. After one hour the reaction mixture was analyzed and there was no appreciable decrease in concentration of phenol. This confirmed the absence of leaching of the catalyst. This was further confirmed by adding alkaline dimethyl glyxime and bromine water to the filtrate, (which gives wine red coloration with nickel ion). The absence of coloration assured the heterogeneous nature of the catalyst [5,33].

In order to examine the possible reusability of catalyst, used catalyst was washed with ethanol and then with water for several times. After washing, the catalyst was dried at 383 K for 12 h. It was observed that used catalyst sample has same catalytic performance as fresh sample (59% degradation of 0.71 M phenol in one hour). In another test the used catalyst was used as such, without washing. It also maintain its activity, but to lesser extent (50% degradation of 0.71 M phenol in one hour). The observed results clearly confirmed the high efficiency of the present process for the facile and convenient degradation of phenol in presence of easily separable and reusable nickel hydroxide catalyst.

3.3. Effect of partial pressure of oxygen

The system was tested in relation to the effect of partial pressure of oxygen on degradation of phenol in the range of 51–101 kPa partial pressure of oxygen. These experiments were performed over nickel hydroxide catalyst at 323 K with 0.71 M initial concentration of phenol and 0.2 g of the catalyst loading. Fig. 5 indicates that oxidation/degradation of phenol increases with partial pressure of oxygen. For determination of various partial pressure of oxygen, nitrogen was admixed with oxygen having the total flow rate of 60 mL min⁻¹. The partial pressure of oxygen was calculated by following expression [34]:

$$p_{O_2} = \frac{F_{O_2}}{F_{O_2} + F_{N_2}} \times 101.2 \text{ kPa}, \quad (4)$$

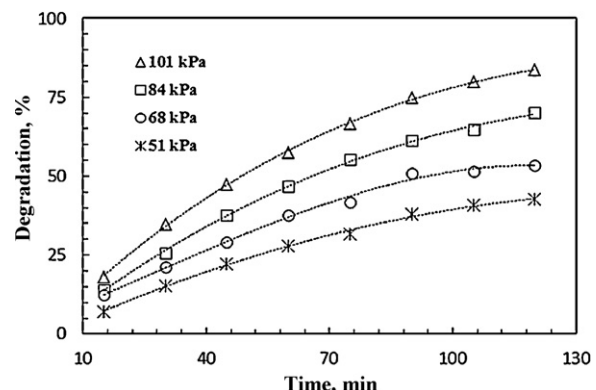


Fig. 5. Time profile of oxidation/degradation of phenol over nickel hydroxide catalyst at various partial pressures of oxygen. Reaction conditions: Phenol 0.71 M (15 mL), Temperature 323 K, Catalyst 0.2 g, Stirring speed 600 rpm.

where F_{O_2} and F_{N_2} represent the flow rate of oxygen and nitrogen, respectively.

3.4. Effect of initial concentration

Fig. 6 shows the % degradation of phenol versus time curves with different initial phenol concentrations at 323 K temperature and 101 kPa partial pressure of oxygen over 0.2 g of catalyst. As the initial concentration of phenol increases, the degradation decreases. It is assumed that as the initial phenol concentration increases, the imposed catalyst loading along with the fixed agitation speed does not allow a complete conversion of phenol, due to mass transfer limitations between gas phase and liquid phase and transport limitations of phenol to the catalyst surface. The effect of decrease in conversion of phenol with increase in initial concentration of phenol can be indicative of some kind of phenol self-inhibition, i.e. of partial deactivation by phenol or transport limitations of phenol to the catalyst surface. For this reason the effect of the catalyst loading and stirrer speed have been investigated. Similar investigations have been reported by C. Resini et al. [18].

3.5. Effect of catalyst loading

The influence of catalyst loading was investigated in the range of 0.05–0.3 g of catalyst loading at the same initial phenol concentration (0.71 M). The temperature was maintained fixed at 323 K and pressure at 101 kPa while stirring the mixture at 600 rpm stirring speed. The results are shown in Fig. 7. The % conversion of phenol increases with increase of catalyst loading in the range of

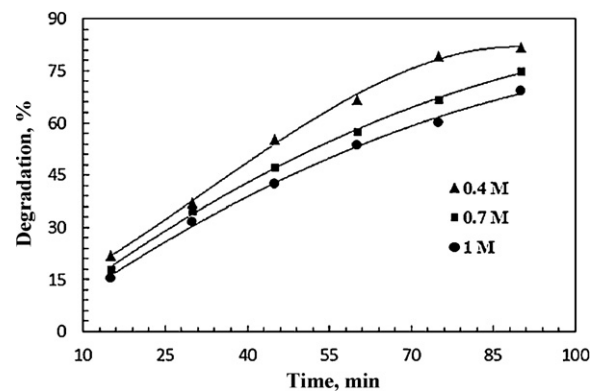


Fig. 6. Time profile of oxidation/degradation of phenol over nickel hydroxide catalyst at various initial concentrations of phenol. Reaction conditions: Temperature 323 K, Partial pressure of oxygen 101 kPa, Catalyst 0.2 g, Stirring speed 600 rpm.

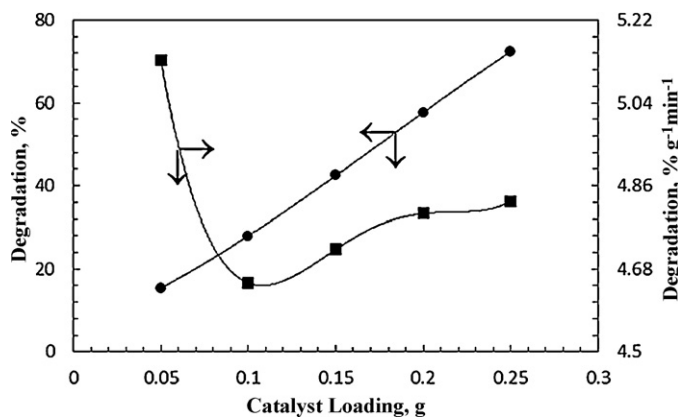


Fig. 7. Effect of catalyst loading on oxidation/degradation of phenol over nickel hydroxide. Reaction conditions: Phenol 0.71 M, Partial pressure of oxygen 101 kPa, Temperature 323 K, Time 60 min, Stirring speed 600 rpm.

0.05–0.35 g; however, the % conversion of phenol per gram of the catalyst per minute decreases with initial increase of catalyst loading from 0.05 to 0.1 g. At higher catalyst load (0.15–0.25 g) the % conversion of phenol per gram of catalyst per minute became almost constant. The behavior of phenol degradation at catalyst loading lower than 0.15 g suggests transport limitations of phenol to the catalyst surface. At higher catalyst loading (0.15–0.25 g), the reaction rate per gram of catalyst seems to be less affected by catalyst loading, indicating that a kinetic control seems to prevail on transport limitations [15,25]. 0.2 g was selected as optimum catalyst loading.

3.6. Effect of stirring speed

The oxidative degradation of phenol over nickel hydroxide catalyst is a typical slurry-phase reaction having one liquid reactant (phenol), a gaseous reactant (oxygen) and solid catalyst. In a batch reactor, the mixture was stirred vigorously in order to slurry the catalyst uniformly throughout the liquid. In order to observe the effect of the speed of agitation on the phenol degradation rate, experiments were carried out at different stirring speeds in the range of 100–900 rpm (Fig. 8). As the stirring speed increases from 100 to 600 rpm, the rate of degradation increases indicating the mass transfer regime. From 600 to 900 rpm, no appreciable differences on conversion are detected. Stirring speed of 600 rpm is the threshold value at which the resistance due to phenol mass transfer to the catalyst particle has overcome [25]. Stirring speed on 600 rpm was selected as optimum stirring speed.

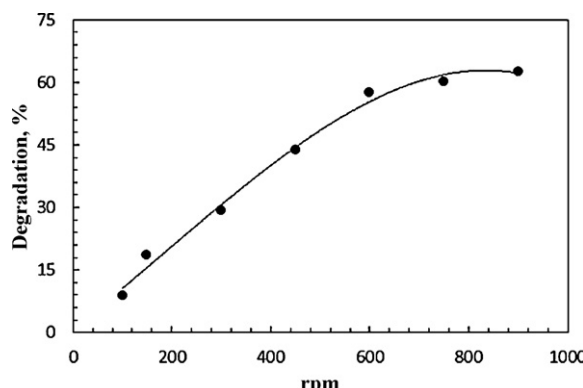


Fig. 8. Effect of stirring speed on oxidation/degradation of phenol over nickel hydroxide. Reaction conditions: Phenol 0.71 M, Partial pressure of oxygen 101 kPa, Catalyst 0.2 g, Temperature 323 K, Time 60 min.

3.7. Kinetic studies

Langmuir–Hinshelwood kinetic model can be used to describe the degradation of phenol catalyzed by nickel hydroxide, in which it is assumed that the reaction between phenol and molecular oxygen is taking place at the surface of catalyst particles. Recently this model has been described for the reaction involving liquid and gaseous reactants at the surface of catalyst, although it was initially developed to describe the reaction involving the gaseous reactants [1,5,7,25,35]. According to Langmuir–Hinshelwood (L–H) theory, first the gaseous molecules of oxygen dissolves into liquid phase and forms dissolved oxygen. Subsequently dissolved oxygen diffuses with aqueous phenol to the catalyst surface and gets adsorbed either in molecular form or in dissociated form. On the surface of catalyst, the adsorbed oxygen and phenol commence the catalytic reaction and generate a number of products. Finally, the products desorb from the surface. This whole process can be summarized in the following steps:

1. $\text{PhOH} + \theta \rightarrow \theta_{\text{PhOH}}$ Adsorption of phenol
2. $\text{O}_2 + \theta \rightarrow \theta_{\text{O}_2}$ Adsorption of molecular oxygen
3. $\text{O}_2 + 2\theta \rightarrow 2\theta_{\text{O}}$ Adsorption of dissociative oxygen
4. $\theta_{\text{PhOH}} + \theta_{\text{O}_2} (\text{or } 2\theta_{\text{O}}) \rightarrow \theta_p$ Catalytic surface reaction
5. $\theta_p \rightarrow P$ Desorption of products

where θ represents the surface active sites.

According to Langmuir–Hinshelwood kinetic theory, the rate of reaction is proportional to the fraction of the surface covered by substrate, θ :

$$\text{Rate} = k_r \theta_{\text{PhOH}} \theta_{\text{O}_2}, \quad (5)$$

where k_r , θ_{PhOH} and θ_{O_2} represents rate constant, surface covered by phenol and molecular oxygen respectively. Unit of rate constant is min^{-1} .

Adsorption of phenol and oxygen on the surface of catalyst may take place either according to Langmuir, Temkin or Freundlich adsorption isotherm. Langmuir adsorption isotherm may be either competitive or non-competitive. For competitive Langmuir adsorption of phenol and oxygen, the rate of reaction can be expressed as:

$$\text{Rate} = k_r \frac{K_{\text{PhOH}} [\text{PhOH}] K_{\text{O}_2}^n [\text{O}_2]^n}{(1 + K_{\text{PhOH}} [\text{PhOH}] + K_{\text{O}_2}^n [\text{O}_2]^n + K_p [P])^2}. \quad (6)$$

K_{PhOH} , $K_{\text{O}_2}^n$ and K_p represent adsorption coefficient for phenol, oxygen and products, respectively. The value of n can be taken 1 or 0.5 for molecular or dissociative adsorption of oxygen, respectively.

Adsorption/desorption processes in the above steps are fast enough to be assumed at equilibrium. This assumption helps to simplify the above expression as:

$$\text{Rate} = k_r \frac{K_{\text{PhOH}} [\text{PhOH}] K_{\text{O}_2}^n [\text{O}_2]^n}{(1 + K_{\text{PhOH}} [\text{PhOH}] + K_{\text{O}_2}^n [\text{O}_2]^n)^2}. \quad (7)$$

If O_2 is kept constant, and combine all the constants together, equation (7) can be modified to:

$$\text{Rate} = \frac{ab[\text{PhOH}]}{(c + b[\text{PhOH}])^2}, \quad (8)$$

where a , b and c are $k_r K_{\text{O}_2}^n [\text{O}_2]^n$, K_{PhOH} and $1 + K_{\text{O}_2}^n [\text{O}_2]^n$, respectively.

Similarly if concentration of phenol is kept constant, equation (7) is transformed to:

$$\text{Rate} = \frac{ab[\text{O}_2]^n}{(c + b[\text{O}_2]^n)^2}. \quad (9)$$

For non-competitive adsorption of phenol and oxygen at the surface of catalyst, the rate expression is

$$\text{Rate} = k_r \frac{K_{\text{PhOH}}[\text{PhOH}]K_{O_2}^n [\text{O}_2]^n}{(1 + K_{\text{PhOH}}[\text{PhOH}](1 + K_{O_2}^n [\text{O}_2]^n)^n)}. \quad (10)$$

For constant pressure of oxygen and concentration of phenol, rate expressions are given by equation (11) and (12), respectively.

$$\text{Rate} = \frac{ab[\text{BzOH}]}{1 + b[\text{BzOH}]}, \quad (11)$$

$$\text{Rate} = \frac{ab[\text{O}_2]}{1 + b[\text{O}_2]}. \quad (12)$$

Considering Temkin adsorption isotherm, the rate expression is given by:

$$\text{Rate} = k_r(K_1 \ln K_2[\text{BzOH}])(\bar{K}_1 \ln \bar{K}_2[\text{O}_2]^n), \quad (13)$$

where K_1 and K_2 are constants related to heat of adsorption, which decreases linearly with surface coverage.

For constant pressure of oxygen and phenol concentration, the rate equations are modified as equations (14) and (15), respectively.

$$\text{Rate} = \bar{k}_r(K_1 \ln K_2[\text{PhOH}]) \quad (14)$$

$$\text{Rate} = \bar{k}_r(K_1 \ln \bar{K}_2[\text{O}_2]). \quad (15)$$

Plot of $\ln[\text{PhOH}]$ or $\ln[\text{O}_2]$ against rate gives straight line.

Similarly considering Freundlich adsorption isotherm, rate of reaction is given by:

$$\text{Rate} = k_r K_{\text{PhOH}}[\text{PhOH}]^{1/n} K_{O_2}[\text{O}_2]^{1/n}, \quad (16)$$

where K_{PhOH} and K_{O_2} are the adsorption coefficient for phenol and oxygen, respectively, and $n (>1)$ is a constant.

This equation can be simplified by keeping pressure of oxygen or concentration of phenol constant as equations (17) and (18), respectively.

$$\text{Rate} = \bar{k}_r K_{\text{PhOH}}[\text{PhOH}]^{1/n} \quad (17)$$

$$\text{Rate} = \bar{k}_r K_{O_2}[\text{O}_2]^{1/n} \quad (18)$$

Plot of $\ln[\text{PhOH}]$ or $\ln[\text{O}_2]$ against \ln rate gives straight line. It is not necessary that both the reactants will adsorb on the surface according to same adsorption isotherm. Phenol and oxygen may follow different adsorption isotherms. Under this condition the rate expression may have various forms.

Time profile data at various temperatures from Fig. 4 was subjected to kinetic analysis according to Langmuir, Temkin and Freundlich models by linear and non-linear least-square method. For non-linear least-square method Curve Expert 1.4 software was used. Rate of the reaction was calculated by applying third order polynomial to the time profile data, using Curve Expert software. Competitive Langmuir model [equation (8)] was applicable to the data indicating that there is a competition between phenol and oxygen for adsorption sites at the surface of the catalyst. Application of Langmuir model indicates that the adsorption of phenol at the surface of catalyst takes place at homogenous surface with infinite number of identical cites. Before applying the kinetic model [equation (8)], it was integrated using Wolfram Mathematica Online Integrator. Integrated form of equation (8) is equation (19), where 0.71 is the initial molar concentration of phenol.

$$t = (a \times (0.71 - x) \times (4 \times b + a \times (0.71 - x)) + 2 \times b^2 \times \ln(0.71/x))/(2 \times c). \quad (19)$$

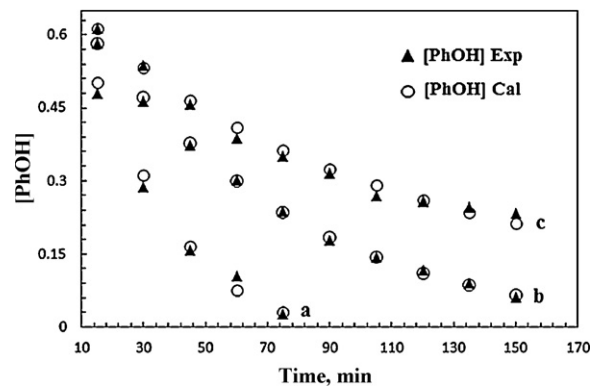


Fig. 9. Fitting of competitive Langmuir model [(equation (8))] to the time profile data at various temperatures.

Table 1

Kinetic constants determined by non-linear least-square analysis according to Langmuir–Hinshelwood, competitive model [(equation (8))].

T, K	$a = k_r K_{O_2} p_{O_2} = k'_r$ (mol L ⁻¹ min ⁻¹)	$b = K_{\text{PhOH}}$ (L mol ⁻¹)	c^a	R^2
313	0.464	0.298	0.111	0.947
323	0.468	0.261	0.219	0.998
333	0.532	0.145	0.981	0.994

^a $c = 1 + K_{O_2} p_{O_2}$ is a unit less quantity.

Fig. 9 shows the fitting of Langmuir competitive model. Values of various constants were determined using Curve Expert software and are listed in Table 1.

Similarly the time profile data at various partial pressures (51–101 kPa) from Fig. 5 was also subjected to kinetic analysis using Langmuir competitive kinetic model. Values of various constants were determined using Curve Expert software and are listed in Table 2.

To investigate the nature of adsorption of oxygen at the surface of catalyst, rate constants at various partial pressure of oxygen listed in Table 2 were subjected to kinetic analysis according the discussed model using Curve Expert software. It was noted that only Temkin model [equation (15)] was applicable to the data, as given in Fig. 10. The slope of the plot is true rate constant, which is 0.1451 min⁻¹.

Some of the researchers have described the kinetic model, where the adsorption term is neglected [35–39]. Basically the catalytic reactions are described with surface concentrations; however, the effect of surface concentrations on rates of reactions can be eliminated by using simplifying assumptions, such as quasi-equilibrium and quasi-steady state hypotheses [18]. Thus neglecting the adsorption term, the overall rate expression can be written as:

$$-\frac{d[\text{PhOH}]}{dt} = K_r(p_{O_2})[\text{PhOH}], \quad (20)$$

Table 2

Kinetic constants determined by non-linear least-square analysis according to Langmuir–Hinshelwood, competitive model [(equation (8))].

p_{O_2} , kPa	$a = k_r K_{O_2} p_{O_2} = k'_r$ (mol L ⁻¹ min ⁻¹)	$b = K_{\text{PhOH}}$ (L mol ⁻¹)	c^a	R^2
51	0.368	0.320	0.077	0.950
68	0.396	0.292	0.105	0.941
84	0.430	0.278	0.156	0.982
101	0.468	0.262	0.219	0.998

^a $c = 1 + K_{O_2} p_{O_2}$ is a unit less quantity.

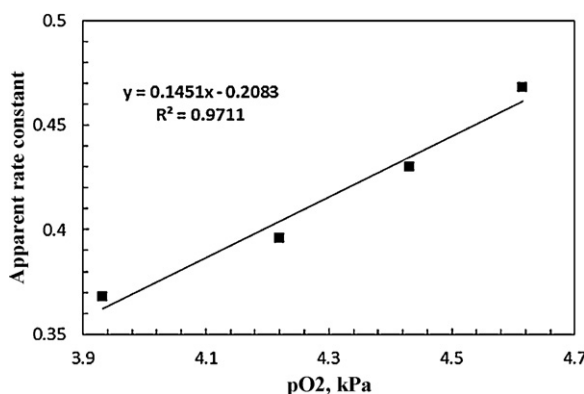


Fig. 10. Fitting of Temkin model [(equation (15))] to the rate at various partial pressure of oxygen.

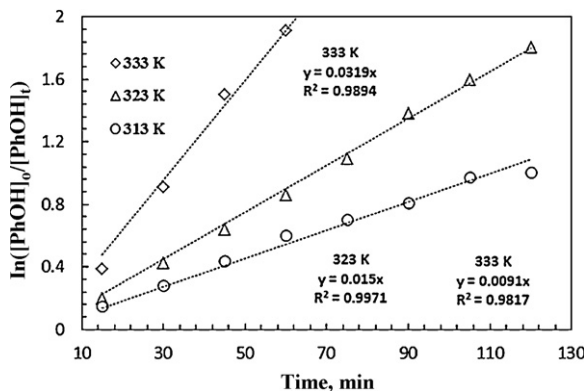


Fig. 11. Fitting to kinetic model 22 to the time profile data at various temperatures.

where K_r is rate constant. It is not the same as given in equation (5). In case of constant pressure of oxygen, equation (20) can be transformed to equation (21):

$$-\frac{d[PhOH]}{dt} = k_r[PhOH], \quad (21)$$

where k_r is the apparent rate constant, which is different than k_f given in equation (5). On rearrangement and integration equation (21) gives equation (22), first order rate equation.

$$\ln \frac{[PhOH]_0}{[PhOH]_t} = k_r t, \quad (22)$$

where $[PhOH]_0$ is initial concentration and $[PhOH]_t$ is concentration of phenol at time t .

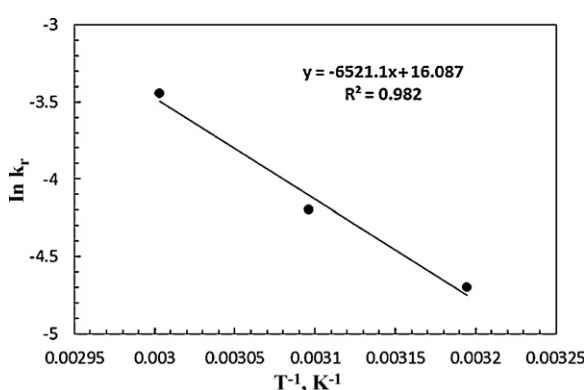


Fig. 12. Arrhenius plot.

The time profile data at various temperatures was subjected to kinetic analysis according to kinetic equation 22 as well. The results are given in Fig. 11. Apparent rate constants were calculated from the slope of the plots. Activation energy was calculated by plotting rate constants versus T^{-1} (Arrhenius plot, as given in Fig. 12). Activation energy was found as 54.2 kJ mol^{-1} . A.J. Luna et al. [14] and Q. Wu et al. [40] have also reported linear plot with three points. This activation energy is in accordance with 54.3 and 48.4 kJ mol^{-1} reported by A.J. Luna et al. [14] and Z.Y. Ding et al. [41], respectively.

4. Conclusions

Nickel hydroxide has demonstrated its efficiency for the phenol degradation. Thus, nickel hydroxide can be considered as effective catalyst for abatement of phenol in aqueous medium. Temperature and partial pressure of oxygen greatly affect the catalytic removal of phenol. The degradation of phenol catalyzed by nickel hydroxide in present case is taking place in kinetic controlled region, where Langmuir–Hinshelwood type of mechanism is operative. According to this mechanism reaction proceed in two steps. In first step both the reactants i.e. phenol and oxygen are adsorbed at the surface of catalyst, while in the second step the adsorbed reactants react and give the final products. Adsorption of phenol and oxygen is taking place according to competitive Langmuir adsorption isotherm and Temkin adsorption isotherm respectively. It shows that the adsorption sites for phenol and oxygen are homogeneous and heterogeneous in nature, respectively. Although the adsorption sites for phenol and oxygen are different, however, oxygen affects the adsorption of phenol. The overall kinetic expression can be concluded as:

$$\text{Rate} = k_r \left(\frac{K_{PhOH}[PhOH]}{(1 + K_{PhOH}[PhOH] + K_{O_2}[O_2]_g^n)^2} \right) (K_1 \ln(K_2 pO_2)).$$

Acknowledgments

Higher Education Commission (HEC) Pakistan is acknowledged for providing financial assistance under Indigenous PhD 5000 and IPFP Program (Muhammad Saeed).

References

- M. Saeed, M. Ilyas, M. Siddique, Journal of the Chemical Society of Pakistan 34 (2012) 626–633.
- D. Rajkumar, K. Planivelu, Industrial and Engineering Chemistry Research 42 (2003) 1833–1841.
- R. Qadeer, A. Rehan, Turkish Journal of Chemistry 26 (2004) 357–361.
- S.T. Hussain, S. Jamil, M. Mazhar, Environmental Science & Technology 30 (2009) 511–524.
- M. Ilyas, M. Saeed, Journal of the Chemical Society of Pakistan 31 (2009) 526–533.
- M. Ilyas, M. Sadiq, Chinese Journal of Chemistry 26 (2008) 941–946.
- M. Ilyas, M. Sadiq, Chemical Engineering & Technology 30 (2007) 1391–1397.
- D.H. Bremner, R. Molina, F. Martinez, J.A. Melero, Y. Segura, Applied Catalysis B: Environmental 90 (2009) 380–388.
- C. Ngamsopasiriskun, S. Charnsethikul, S. Thachepon, A. Songsasen, Kasetsart Journal (Natural Science) 44 (2010) 1176–1182.
- N.A. Laoufi, D. Tassalit, F. Bentahar, Global Nest Journal 10 (2008) 404–418.
- W. Wang, P. Serp, P. Klack, J.L. Faria, Journal of Molecular Catalysis A: Chemical 235 (2005) 194–199.
- Z. Wang, W. Cai, X. Hong, X. Zhao, F. Xu, C. Cai, Applied Catalysis B: Environmental 57 (2005) 223–231.
- H. Wang, J. Li, X. Quan, Y. Wu, G. Li, F. Wang, Journal of Hazardous Materials 141 (2007) 336–343.
- A.J. Luna, L.O.A. Rojas, D.M.A. Melo, J.F. Benachour, M. de Sousa, Brazilian Journal of Chemical Engineering 26 (2009) 493–502.
- T.L. Lai, C.C. Lee, K.S. Wu, Y.Y. Shu, C.B. Wang, Applied Catalysis B: Environmental 68 (2006) 147–153.
- T.L. Lai, Y.L. Lai, C.C. Lee, Y.Y. Shu, C.B. Wang, Catalysis Today 131 (2008) 105–110.
- G. Ovejero, S.L. Sotelo, J. Garcia, A. Rodriguez, Journal of Chemical Technology & Biotechnology 80 (2005) 406–410.

- [18] C. Resini, F. Catania, S. Berardinelli, O. Paladino, G. Busca, *Applied Catalysis B: Environmental* 84 (2008) 678–683.
- [19] J.A. Melero, G. Calleja, F. Martínez, R. Molina, M.I. Pariente, *Chemical Engineering Journal* 131 (2007) 245–256.
- [20] K. Nakagawa, R. Konaka, T. Nakata, *The Journal of Organic Chemistry* 27 (1962) 1597–1601.
- [21] R. Konaka, S. Terabe, K. Kuruma, *The Journal of Organic Chemistry* 34 (1969) 13341–13345.
- [22] S. Christoskova, N. Danova, M. Georgieva, O.K. Argirov, D. Mehandzhiev, *Applied Catalysis A: General* 128 (1995) 219–229.
- [23] S. Christoskova, M. Stoyanova, *Water Research* 36 (2002) 2297–2303.
- [24] H. Ji, T. Wang, M. Zhang, Y. She, L. Wang, *Applied Catalysis A: General* 128 (1995) 219–225.
- [25] M. Ilyas, M. Saeed, *International Journal of Chemical Reactor Engineering* 8 (2010) A77.
- [26] G. Wu, T. Jeong, C. Won, L. Cui, *Korean Journal of Chemical Engineering* 27 (2010) 168–173.
- [27] G.P. Glaspell, P.W. Jadodzinski, A. Manivannan, *The Journal of Physical Chemistry B* 108 (2004) 9604–9607.
- [28] C. Hu, S. Xing, J. Qu, H. He, *The Journal of Physical Chemistry C* 112 (2008) 5978–5983.
- [29] Y. Hu, H. Kondoh, M. Shimojo, T. Kogure, T. Ohta, *The Journal of Physical Chemistry B* 109 (2005) 19094–19098.
- [30] J. Arana, C.G. Cabo, J.M. Dona-Rodríguez, O.G. Diaz, J.A. Herrera-Melian, J. Perez-Peña, *Applied Surface Science* 239 (2004) 60–71.
- [31] C. Ehrhard, M. Gjikaj, W. Brockner, *Thermochimica Acta* 432 (2005) 36–40.
- [32] R. Xu, H. Zeng, *The Journal of Physical Chemistry B* 107 (2003) 926–930.
- [33] G. Charlot, *Colorimetric Determination of Elements. Principles and Methods*, Elsevier Publishing Company, Amsterdam, 1964.
- [34] M. Ilyas, M. Saeed, *International Journal of Chemical Reactor Engineering* 9 (2011) A75.
- [35] Q. Hu, X. Hu, P.L. Yue, *International Journal of Chemical Reactor Engineering* 3 (2005) A29.
- [36] P.M. Alvarez, D. McLurgh, P. Plucinski, *Industrial and Engineering Chemistry Research* 41 (2002) 2147–2152.
- [37] P.M. Alvarez, D. McLurgh, P. Plucinski, *Industrial and Engineering Chemistry Research* 41 (2002) 2153–2158.
- [38] A. Pintar, J. Levec, *Industrial and Engineering Chemistry Research* 33 (1994) 3070–3077.
- [39] P.D. Vaidya, V.V. Mahajani, *Chemical Engineering Journal* 87 (2002) 403–416.
- [40] Q. Wu, X. Hu, P.L. Yue, *International Journal of Chemical Reactor Engineering* 3 (2005) A29.
- [41] Z.Y. Ding, S.N.V.K. Aki, *Environmental Science & Technology* 29 (1995) 2748–2754.